Title
The diagnosis of limbal stem cell deficiency

Journal
The Ocular Surface, 16(1)

ISSN
1542-0124

Authors
Le, Qihua
Xu, Jianjiang
Deng, Sophie X

Publication Date
2018

DOI
10.1016/j.jtos.2017.11.002

Peer reviewed

HHS Public Access

Author manuscript

Ocul Surf. Author manuscript; available in PMC 2019 January 01.

Published in final edited form as:

Ocul Surf. 2018 January ; 16(1): 58–69. doi:10.1016/j.jtos.2017.11.002.

Review. The diagnosis of limbal stem cell deficiency

Qihua Le, MD, PhD[a,b], **Jianjiang Xu, MD, PhD**[b], and **Sophie X. Deng, MD, PhD**[a,*]

[a]Stein Eye Institute, Cornea Division, David Geffen School of Medicine, University of California, Los Angeles

[b]Department of Ophthalmology, Eye & ENT Hospital of Fudan University, Shanghai 200031, China

Abstract

Limbal stem cells (LSCs) maintain the normal homeostasis and wound healing of corneal epithelium. Limbal stem cell deficiency (LSCD) is a pathologic condition that results from the dysfunction and/or an insufficient quantity of LSCs. The diagnosis of LSCD has been made mainly based on medical history and clinical signs, which often are not specific to LSCD. Methods to stage the severity of LSCD have been lacking. With the application of newly developed ocular imaging modalities and molecular methods as diagnostic tools, standardized quantitative criteria for the staging of LSCD can be established. Because of these recent advancements, effective patient-specific therapy for different stages of LSCD may be feasible.

Keywords

Anterior-segment optical coherence tomography; Conjunctival marker; Diagnosis; Impression cytology; In vivo confocal microscopy; Limbal stem cell deficiency; Molecular marker

1. Introduction

Limbal stem cells (LSCs) are adult stem cells that further differentiate into corneal epithelium. Functional LSCs are essential for maintaining the integrity of the corneal surface and transparency of the cornea. The limbus is the transition area between the transparent cornea and the opaque sclera [1]. Normal limbus and LSCs act as a barrier against the invasion of conjunctival epithelial cells onto the cornea [2–4]. In the past four decades, most studies of LSCD have focused on the biology of LSCs and their function in maintaining the regeneration of the corneal epithelium under healthy and pathologic conditions.

LSCs reside in the basal layer of epithelium within the limbal area [5, 6]. Studies have provided direct evidence of LSC survival and self-maintenance at the limbus by using

*Corresponding author: Sophie X. Deng, MD, PhD, Stein Eye Institute, University of California, Los Angeles, 100 Stein Plaza, Los Angeles CA 90095, USA, deng@jsei.ucla.edu, Telephone: (310) 206-7202, Fax: (310) 794-7906.

The authors have no commercial or proprietary interest in any concept or product described in this article.

transgenic mice that expressed ubiquitous green fluorescent protein [7, 8]. The palisades of Vogt, a limbal structure that is shown to harbor a high density of LSCs, provide the niche microenvironment that is necessary for the survival and function of LSCs, and maintenance of their stemness. It might represent the collective influence of coexisting local stromal cells, the extracellular matrix, local vasculature and soluble growth factors [4, 6, 9–12]. LSCs are also found outside of the palisades of Vogt in adult and fetal human eyes, including limbal epithelial crypts and limbal epithelial pit [7, 13, 14].

Direct damage to LSCs and/or the destruction of their niche microenvironment leads to limbal stem cell deficiency (LSCD). As a result, the barrier function of the limbus is compromised, and the corneal epithelium is replaced with conjunctival epithelial cells, which is the hallmark of LSCD. Neovascularization could occur within the corneal epithelium and stroma, and the cornea becomes opaque eventually, leading to vision loss and blindness [3, 15].

Accurate diagnosis of LSCD is crucial because appropriate treatments can prevent progression of the condition and further damage to the ocular surface. For example, penetrating keratoplasty cannot restore sight to an eye blinded by LSCD before functional LSCs are restored [16]. In the past several decades, diagnosis of LSCD was predominantly made based on the patient's medical history and clinical signs. However, inherent limitations are associated with the interpretation of clinical signs [17]. For instance, the presence of a fibrovascular pannus may be caused by previous infectious keratitis rather than LSCD. Moreover, there is no consensus on the methods to stage the severity of LSCD. With the application of newly developed ocular imaging techniques and progress in identifying molecular diagnostic markers and developing new tests based on these markers, the diagnosis of LSCD is coming into a new era.

To review the recent advances in the diagnosis of LSCD, we performed a systematic search on PubMed for English language literature published before March 31, 2017. The following combined search terms were used: "limbal stem cell deficiency" AND "diagnosis," "limbal stem cell deficiency" AND "in vivo confocal microscopy," "limbal stem cell deficiency" AND "optical coherence tomography," "limbal stem cell deficiency" AND "impression cytology." Publications that are not related to the diagnosis of LSCD, or are published in non-English language were excluded. We collected data on diagnostic methods (clinical findings, in vivo confocal microscopy, anterior segment optical coherence tomography [OCT], impression cytology, or detection for various epithelial molecular markers). This literature review summarizes the diagnostic methods currently used in the diagnosis of LSCD and reports recent advances in the diagnosis and classification of LSCD. Based on these findings, a diagnostic approach for LSCD is proposed in the near future to overcome the limitations using the current diagnostic methods. We hope that this review will further emphasize the need to include objective testing using in vivo imaging modalities.

2. Etiology

The two pathologic mechanisms of LSCD are the direct destructive loss of LSCs and the loss of the limbal microenvironment/niche needed for LSC survival. The delicate niche of

LSCs plays an important role in maintaining the LSC pool. Pathologic processes leading to either the direct loss of the LSC pool or the dysfunction of the limbal niche can result in the same phenotype of LSCD.

The etiology of LSCD can be primary, resulting from genetic mutations that lead to LSC dysfunction or destruction. The known causes of primary LSCD include aniridia [18, 19], congenital epidermal dysplasia [20, 21], dyskeratosis congenital [22], keratitis associated with multiple endocrine deficiencies [3], Turner syndrome [23], lacrimo-auriculo-dento-digital (LADD) syndrome [24], and xeroderma pigmentosum [25].

LSCD can also be secondary, resulting from external factors that directly destroy LSCs, damage the stem cell niche, or both. Common causes include chemical or thermal injuries [5, 15, 26–28]; chronic inflammation and cicatricial process from mucous membrane pemphigoid [28, 29], Stevens-Johnson syndrome [30, 31], graft-versus-host disease [32] and chronic limbitis [33, 34]; iatrogenic injury caused by ocular surgeries, radiation, cryotherapy, or systemic chemotherapy [28, 35–38]; drug-induced toxicity such as that caused by mitomycin C, 5-fluorouracil, and sulfur mustard [39–41]; and contact lens wear [28, 42, 43]. LSCD secondary to other ocular surface disorders has also been reported; these disorders include extensive microbial infection [28], neurotrophic (neural and ischemic) keratopathy [44], bullous keratopathy [45], and extensive ocular surface tumors [46].

Animal models have been established to investigate the pathogenesis of LSCD. Transcription factor PAX6 (paired box 6) is critical in anterior segment and corneal development. Mutations in PAX6 lead to aniridia and LSCD both in humans and mice [47, 48]. In the $Pax6^{+/-}$ mouse model with heterozygous $Pax6^{+/Sey\text{-}Neu}$ mutant allele on a congenic CBA/Ca genetic background, unstable corneal homeostasis and features of progressive corneal deterioration are observed. This mouse model has been used to investigate the effect of *Pax6* genotype and age on corneal epithelial cells and to explore the pathogenesis of LSCD [49]. Another mouse model of LSCD was created by using topical administration of benzalkonium chloride at high concentrations [50]. Sulfur mustard exposure induces severe ocular injury and late-onset LSCD in humans. Both rabbit [51] and mouse [52] models of sulfur mustard gas injury have been created. Information obtained from studies of these animal models will shed light on different mechanisms by which LSCD develops and aid in the development of appropriate treatments for LSCD arising from different causes.

3. Clinical presentations

3.1. Symptoms

Patients suffering from LSCD may present with a wide variety of symptoms related to poor epithelial wound healing and recurrent erosions. Patients often experience chronic conjunctival redness, decreased vision, photophobia, foreign body sensation, tearing, blepharospasm, and recurrent episodes of pain from recurrent epithelial breakdown. The pain, photophobia, and discomfort are often debilitating. However, most of these symptoms are nonspecific and inadequate to make the diagnosis correctly.

3.2. Clinical findings under slit-lamp biomicroscopy

Slit-lamp biomicroscopy has been the most commonly used method to make the diagnosis of LSCD. Examination under white light without fluorescein staining provides very limited information to make a correct diagnosis of LSCD. Examination under cobalt blue light using fluorescein staining is essential to detect the subtle signs of LSCD, particularly in the mild or early stage of LSCD (Figs. 1F and 1G).

LSCD may be progressive or stationary, diffuse or sectoral (partial). Clinical manifestations of LSCD vary depending on the severity and extent of limbal involvement.

3.2.1. Mild stage—In the mild stage of LSCD, slit-lamp examination findings include dull/irregular corneal surface with loss of light reflex, corneal epithelial opacity and loss of limbal palisades of Vogt.

3.2.1.1. Epithelial opacity: Compared with transparent corneal epithelium seen in normal cornea (Figs. 1A and 1B), a dull and irregular reflex of the epithelium that varies in thickness and transparency [53] is usually seen on the affected corneal surface. These abnormal epithelial cells may be a mixture of metaplastic corneal epithelial cells and conjunctival epithelial cells, or only conjunctival epithelial cells without neovascularization [54, 55]. The irregular opacified epithelium can be identified under white light with careful examination, but is better visualized using fluorescein staining under cobalt blue light.

3.2.1.2. Epithelial staining: Fluorescein allows visualization of the abnormal cells and their pattern of distribution under cobalt blue light. Fluorescein tends to pool on the affected area because the abnormal conjunctival/metaplastic epithelium layer tends to be thinner and lacks cell-cell tight junctions [56]. The late staining on the abnormal area remains after 10 minutes and can be visualized even after rinsing with balanced salt solution or eye wash. In the mild or early stage of LSCD, stippled fluorescein staining may be present [43, 53]. As the disease becomes more severe, a clear line of demarcation may sometimes, but not always, be visible between the area covered by the corneal and conjunctival epithelial cells in sectoral LSCD (Figs. 1F and 1G).

3.2.1.3. Loss of palisades of Vogt: The palisades of Vogt are more commonly seen in the superior and inferior limbus. In the early or mild stage of LSCD, there may be flattening at the limbus in the region of palisades of Vogt or loss of palisades of Vogt. However, this presentation is not reliably found in all cases. Loss of palisades is also age-related [57].

3.2.2. Moderate stage—A common feature of moderate stage LSCD is fluorescein staining and epithelial thinning in a vortex pattern. Superficial neovascularization and peripheral pannus may be present. The extent of LSCD can range from sectoral to total involvement of the limbus. If the central visual axis is involved, the vision can be significantly compromised.

3.2.2.1. Vortex keratopathy: In the moderate or intermediate stage of LSCD, the abnormal epithelium forms a confluent sheet spreading in a spiral pattern from the limbus onto the cornea and invading the visual axis occasionally (Fig. 1K). With fluorescein staining, a

whorl or vortex pattern of abnormal epithelium can be visualized (Fig. 1L). Sometimes it is referred to as *whorl-like epitheliopathy* [42, 53, 55], which is typically present in the moderate stage. The abnormal epithelium is prone to erosion, and mild anterior stromal haze may be present in the area affected by LSCD.

3.2.2.2. Superficial vascularization and peripheral pannus: Limbal stem cells and corneal epithelium play a significant role in maintaining the angiogenic balance in favor of avascularity [58]. Conjunctival epithelial cells, which migrate onto the cornea in LSCD, have been shown to attract new vessels and they may lack the ability to secrete certain anti-angiogenic factors found in normal corneal epithelium [56]. Therefore, superficial vascularization of the cornea and peripheral pannus are usually seen in the moderate stage of LSCD [54, 59].

3. 2.3. Severe stage—Recurrent or persistent corneal epithelial defect, corneal neovascularization, corneal stroma scarring and opacification are often present in severe-to-total LSCD.

3.2.3.1. Recurrent/persistent epithelial defects: As the population of functional LSCs declines further, recurrent or persistent epithelial defects often occur (Fig. 1Q). Chronic non-healing corneal epithelial defect or repeated epithelium breakdown followed by slow healing are common clinical manifestations of LSCD. Because of the compromised corneal epithelial barrier, the risk of microbial infection increases [60, 61]. Corneal melt or even perforation that may or may not be related to infection can occur in severe LSCD as a result of the persistent epithelial defect.

3.2.3.2. Stromal neovascularization: Both persistent epithelial defects and deteriorated barrier function of the limbus might contribute to an ingrowth of fibrovascular pannus and neovascularization at deep stroma. Although stromal neovascularization is common in severe LSCD, it can also be found in other eye disorders without LSCD, such as herpetic keratitis and previous microbial keratitis.

3.2.3.3. Stromal scarring and opacity: Severe-to-total deficiency of functional LSCs results in almost complete absence of normal corneal epithelium. Corneal stromal haze often worsens as a result of the longstanding instability of the epithelial surface (Fig. 1P). Stromal scarring, calcification, and eventual opacification often occur at the end stage of LSCD. The severe corneal epithelial and stromal opacity leads to functional blindness. Sometimes total or partial keratinization of the covering epithelium may be present due to associated aqueous tear deficiency rather than LSCD.

4. Current diagnostic methods

4.1. Clinical examination

As noted in Section 3, clinical findings under slit-lamp biomicroscopy have been the main basis for the diagnosis and classification of LSCD. A detailed description of the clinical presentations presently used to diagnose and classify mild, moderate, and severe/total LSCD is provided above and summarized in Table 1.

Although fluorescein staining is essential in the diagnosis of LSCD, the technique to instill fluorescein into the conjunctival sac is crucial to elicit the clinical signs of LSCD. Briefly, a sterile fluorescein strip is wetted by approximately 20 μL sterile saline solution and instilled into the inferior conjunctival sac without touching the cornea or limbus. Patients are then instructed to blink several times to allow the fluorescein to spread over the entire ocular surface. Too much fluorescein will mask the pathology and too little fluorescein will not stain epithelium sufficiently, thus compromising its diagnostic effect.

4.2. Impression cytology

Impression cytology is a well-established method to diagnose ocular surface diseases [62, 63]. It is performed by applying a cellulose acetate filter paper, nitrocellulose membrane or Biopore membrane to the ocular surface to remove the very superficial layers of ocular surface epithelium. The specimens can be subjected to hematoxylin and eosin (H&E), Periodic acid Schiff, Papanicolaou, or Giemsa staining to evaluate the morphology of cells taken from ocular surface, both goblet cells and epithelial cells. Impression cytology has been used as a standard technique to study squamous metaplasia and goblet cell loss in ocular surface diseases, such as dry eye disease, chemical injuries, cicatrizing conjunctivitis, vitamin A deficiency, and effects of diverse medications [62].

The presence of goblet cells on the cornea indicates the invasion of conjunctival cells, which is a hallmark of LSCD [45, 63–65]. The identification of goblet cells on the specimens taken from corneal surface by impression cytology has been considered as the “gold standard” in the currently used diagnosis system for LSCD. Moreover, impression cytology on the cornea has been used from the first limbal transplantation to evaluate the restoration of corneal phenotype after surgery [66].

The sensitivity of impression cytology in the diagnosis of LSCD is affected by many factors. Filter pore size affects the consistency of cell collection, and the surfactant treatment of the filter paper can reduce cell pick-up. Therefore, surfactant- free filter paper with pore size 0.22–0.44 μm is recommended [63]. Compared to Biopore membrane, cellulose acetate filter paper is easily wetted during the sample acquisition, either from the anesthetic used beforehand and/or reflex tearing, leading to a poorer cell acquisition and staining outcome. The pressure being applied to the membrane also has a direct effect on the number of cells harvested. The more epithelial cells that are sampled, the greater the number of goblet cells detected on the filter/membrane [67]. The location of sampling is also important, especially in sectoral LSCD. Some researchers divide the membrane into two “D” shaped halves or one large round disk (13 mm) to cover the entire corneal and limbal surface, while others use four fan-shaped pieces to achieve better contact between the membrane and ocular surface [63]. Identification of the location where abnormal epithelium is detected is important, especially in cases of sectoral LSCD.

4.3. Limitations of current diagnostic methods

A recent review reported that more than 60% of the interventional studies on LSCD performed from 2003 to 2013 used diagnostic criteria solely based on clinical presentations, and 30% used the combination of clinical signs and impression cytology for the diagnosis of

LSCD [68]. Less than 10% of the interventional studies used the combination of slit-lamp biomicroscopy and other diagnostic tests, such as imaging (e.g., in vivo confocal microscopy [IVCM]) and/or molecular tests to detect conjunctival epithelial cells on the cornea.

Several findings indicate that current diagnostic criteria cannot accurately assess the severity of LSCD [69–71]. Structural changes occur before the onset of clinical signs. Although clinical signs and presentations are important in the diagnosis of LSCD, many signs described above are not pathognomonic of LSCD and can be found in other ocular disorders. In addition, detection of those subtle clinical signs is operator-dependent and interpretation of clinical signs is subjective. Normal variations of the limbal structure can further complicate the interpretation. For instance, the palisades of Vogt signify a normal healthy limbus. Disarrayed or absence of palisades of Vogt may be an early anatomical change in mild LSCD or as a result of normal variant or aging process [72]. Subtle fluorescein staining patterns in sectoral or partial LSCD may be missed by clinical examination. Some signs present in LSCD, such as fine stippling fluorescein staining and corneal neovascularization, are nonspecific and are present in other conditions that do not have a component of LSCD. Previous studies also suggest that changes in the microstructure precede the clinical presentation in LSCD [53, 69]. Therefore, clinical presentations are insufficient to provide quantitative evaluation for grading the severity of LSCD.

Although the presence of goblet cells on the corneal surface signifies conjunctival epithelial invasion, the absence of goblet cells on the cornea does not necessarily exclude the presence of LSCD. In Stevens-Johnson syndrome, advanced mucous membrane pemphigoid and severe chemical burn, the number of goblet cells is decreased on the ocular surface [73–75]. Sensitivity of impression cytology is low in patients with such disorders and may lead to a false-negative result. The sensitivity of impression cytology varies due to a lack of standardization in the collection and cytological staining protocol [76, 77]. Sampling bias exists because of tight junction of corneal epithelial cells. Therefore, impression cytology is not a quantitative test and cannot be used to quantify the severity of LSCD.

It is difficult to distinguish severe LSCD from total LSCD based on the current diagnostic methods. Although the clinical presentations of severe LSCD and total LSCD are similar, their clinical outcome and prognosis after treatment are likely to be different. A recent study found that residual normal limbal epithelial cells were present in eyes that are categorized as total LSCD using the current diagnostic criteria [71]. It has also been observed that the host LSCs reconstructed the corneal epithelium after allogeneic LSC transplantation in a significant number of successful cases [78, 79], suggesting that the residual LSCs in these recipient eyes might be responsible for reconstruction of the normal corneal epithelial surface. The amount of residual functional LSCs likely plays an important role in the clinical outcome of LSCT. Therefore, it is important to distinguish severe LSCD from total LSCD. An accurate diagnosis and staging of LSCD is of paramount importance in the assessment of the efficacy of different treatments for LSCD.

5. Recent advances in the diagnosis of LSCD

To overcome the shortcomings of current diagnostic methods of LSCD, researchers have investigated the utility of newly developed ocular anterior-segment imaging modalities in the diagnosis of LSCD. Moreover, significant progress has been made in identifying molecular markers that can be developed into new diagnostic tests.

5.1. In vivo imaging

5.1.1. In vivo laser scanning confocal microscopy—In vivo laser scanning confocal microscopy (IVCM) is a noninvasive method to visualize the microstructures within the cornea, limbus, and conjunctiva at the single cell level [31, 57, 80–84]. IVCM has a lateral resolution of 1 μm, and axial resolution of 4 μm [85]. The morphology of the corneal epithelium, corneal subbasal nerve plexus, corneal stroma, and limbal structure can be visualized in healthy and abnormal eyes. Hence, the use of IVCM in ophthalmology, especially in the studies of LSCD, has expanded greatly over the last decade [18, 27, 53, 69–71, 80, 86–89].

5.1.1.1 Techniques of IVCM on patients with LSCD: Currently, two types of in vivo confocal microscopes are commercially available: ConfoScan 4 (NIDEK CO., LTD, Japan) and Heidelberg Retina Tomography (HRT) with a cornea module (Heidelberg Engineering GmbH, Germany). With the application of laser as light source, HRT can obtain images of limbus with better quality, thus becoming the main tool in the study of limbus under normal and pathological conditions. Since the typical size of HRT IVCM image is 0.4 x 0.4 mm^2, representing only 0.15% of the total corneal area, careful slit lamp examination before IVCM can help to determine the location of pathology, which is important to obtain images with good diagnostic values, especially in patients with sectoral LSCD. Patient cooperation is also crucial for obtaining good confocal pictures. Detailed explanation to patients before the examination will alleviate their anxiety and fear caused by the direct contact from the confocal lens. To look for residual LSCs in cases of severe-to-total LSCD, a quick scan of the entire 360 degrees of limbus using the “Sequence” mode is preferred. Patients is instructed to rotate their eyes by following the target light to position the limbus to the imaging areas.

5.1.1.2. IVCM parameters for the diagnosis of LSCD: The detection of goblet cells on the cornea by IVCM has been reported as a diagnostic marker of LSCD [64, 88]. However, detection of goblet cells by IVCM is examiner-dependent and has the same limitations as those in impression cytology for the diagnosis of LSCD, as discussed previously [27, 64]. Moreover, there is no consensus in regard to the morphologic features of goblet cells observed on the confocal images. Some studies have reported that goblet cells exhibit a hyper-reflective cytoplasm [77, 90], whereas other studies have suggested that the cytoplasm is hypo-reflective [91]. This variation might be due to the secretion status of the goblet cells. Therefore, new parameters to identify abnormal corneal epithelium, limbal epithelial cells, and conjunctival epithelial cells are more precise and are needed to improve the sensitivity and accuracy of IVCM in the diagnosis of LSCD.

5.1.1.2.1. Corneal and limbal epithelium: Normal corneal epithelium is composed of superficial cells, wing cells, and basal cells. Superficial cells usually appear to be loosely arranged, large hexagonal or polygonal flat cells with hyper-reflective cytoplasm. Wing cells, located between superficial cells and basal cells, have a dark cytoplasm, well-defined bright cell borders, and no visible nuclei (Fig. 1C). Basal epithelial cells are the smallest of the three types of corneal epithelial cells, with a diameter of 8–10 μm [85]. They usually appear as a regular mosaic of dark cell bodies with cell borders visible but less clearly defined than those seen in wing cells. The nuclei of basal epithelial cells are often not visible or very faint. The subbasal nerve plexus is visible at the basal and subbasal layer of corneal epithelial cells in normal eyes (Fig. 1D).

Significant microstructural changes in the corneal epithelium are detected in patients with LSCD, even in those with mild- or early-stage LSCD. The epithelial cells in patients with LSCD have less distinct borders and prominent nuclei (Fig. 1H and 1I). In more advanced stages of LSCD, more morphologic abnormalities of the epithelial cells can be seen (Fig. 1M and 1N). In eyes with severe LSCD, epithelial cells are metaplastic (Fig. 1R and 1S) and neovascularization may be seen. Compared with healthy eyes, eyes with LSCD have significantly decreased basal epithelial cell density (31.0% reduction in LSCD eyes) and larger size of basal epithelial cells (19.7% augmentation in LSCD eyes) [53, 69]. There is a positive correlation between the reduction of basal cell density and the severity of LSCD [69]. Although the morphologic changes of the corneal epithelium are not specific to LSCD, the large-scale reduction of basal cell density has been reported only for LSCD. In addition to the changes in morphology and basal cell density, the epithelial thickness at the central cornea is also decreased significantly in patients with LSCD (20.2% reduction in LSCD eyes) [70]. The extent of epithelial thinning is also positively correlated with the degree of LSCD.

The limbal epithelium undergoes morphologic changes similar to those of the corneal epithelial cells, including decreased cellular density (23.6% reduction in LSCD eyes), enlarged cellular size (13.5% augmentation in LSCD eyes), and alterations in the cell morphology [69, 92]. The epithelial thickness at the limbal area is also significantly reduced (38.5% reduction in LSCD eyes) [70]. Similar to the changes found in the central cornea, the reduction of basal limbal epithelial density and limbal epithelium thickness positively correlates with the severity of LSCD. More importantly, there are significant decreases in basal cell density and epithelial thickness in the limbal regions that do not exhibit clinical signs of LSCD in eyes with sectoral LSCD. This finding suggests that these microstructural changes precede the clinical presentation of LSCD.

5.1.1..2.2 Subbasal nerve plexus: In addition to epithelial cells, the subbasal nerve plexus is affected in LSCD. Innervation of the corneal epithelium plays a pivotal role in the maintenance of health and function of the epithelium. Corneal nerves not only protect the ocular surface through an elaborate mechanism of sensation and blink reflex, but also release various trophic factors that regulate epithelial integrity, proliferation, and wound healing [93, 94].

In patients with LSCD, drastic changes in the morphology and the density of the subbasal nerve plexus are observed, which correlate with the severity of LSCD (Fig. 1I, 1N, 1S). Compared with control subjects, subbasal nerve density was reduced by 34.9% in the early stage, 54.0% in the intermediate stage, and 73.5% in the late stage of LSCD [95]. Other distinct morphologic changes of the subbasal nerve plexus in patients with LSCD include severe nerve dropout, short nerve branches, and sharp turns of the branched nerve [95]. In patients with severe LSCD, such as in mucous membrane pemphigoid [96], chronic Stevens-Johnson syndrome, and toxic epidermal necrolysis [31], the subbasal nerve plexus is usually not detectable.

It should be noted that reduced corneal subbasal nerve density can be found under many pathological conditions, including systemic diseases [97, 98], ocular disorders [99–101], and alterations caused by ocular surgeries or therapies [102–105]. Therefore, this parameter is not specific to LSCD. The sensitivity and specificity of subbasal nerve density in the diagnosis of LSCD requires further investigation.

5.1.1.2.3. Corneal and limbal stroma: The morphology of corneal and limbal stroma is affected in LSCD. A large number of inflammatory and dendritic cells are sometimes present with blood vessels within the epithelial layer and deep stromal layers [33, 106]. The slightly hyper-reflective stroma in normal eyes is replaced by homogenously bright fibrotic structures in LSCD even at mild stage [107].

At the limbal area, the palisades of Vogt may be detected in normal eyes by IVCM. The palisades of Vogt usually appear as hyper-reflective, double-contour, linear structures (Fig. 1E). These structures alternate with islands of epithelial cells that correspond to the inter-palisade rete pegs [80, 82]. In moderately pigmented healthy subjects, a bright fringe of hyper-reflective basal epithelial cells around stromal papilla is usually seen [57]. Limbal projections, which are round cords of stroma that extend into the limbal epithelium, is another structure observed in normal eyes [80, 108].

In patients with LSCD, the structure of the palisades of Vogt is altered or totally absent (Fig. 1J, 1O, 1T) [86, 88, 89]. Limbal projections are often absent. Interestingly, well-demarcated, lacunae-like structures are occasionally found in certain limbal regions of eyes with sectoral LSCD. These structures extend into the deep underlying limbal stroma and contain clusters of highly packed normal limbal epithelial-like cells. These individual structures can extend more than 100 μm into the stroma [109]. The deep location may protect LSCs from surface insults. The exact mechanism by which these lacunae-like structures are formed in sectoral LSCD is unknown.

5.1.1.2.4 Summary: Although the feasibility of using IVCM in the diagnosis of LSCD has been investigated by many researchers [53, 69, 70, 72, 81, 88, 89], the threshold values for the diagnosis in clinical practice cannot be given based on the present studies, because the number of study populations is not large enough. Moreover, basal cell density and epithelial thickness change with age [57, 110]. Therefore, a large study to determine the normal variation due to aging will be necessary to distinguish the degree of change in these two parameters that signify and grade the degree of LSCD. The percentage of reduction or

augmentation from the normal level would be a better index than the actual measurement because there might be the variations in the cell counting among different centers or examiners.

5.1.2. Anterior segment optical coherence tomography

5.1.2.1. Principles: OCT, a noninvasive and noncontact imaging technique that was first introduced in 1994 [111], is based on low-coherence interferometry. It compares the time-delay and intensity of infrared light reflected from the tissue structures against a reference beam. To obtain an OCT image, multiple scans are performed to create a series of axial scans (A-scans), and these A-scans are combined into a composite two-dimensional image, or cross-sectional tomography [112].

Anterior segment OCT (AS-OCT) can image ocular anterior segment structures, including the cornea, limbus, anterior chamber and angle without the use of topical anesthesia. Commercially available AS-OCT systems (Table 2) are developed on two different platforms: time-domain and spectral domain (also called Fourier-domain). In time-domain OCT, cross-sectional images are produced by varying the position of the reference mirror [112]. Spectral domain OCT uses a stationary reference mirror [112]. The signal of interference between the sample and reference reflection is detected by varying the wavelength of the light source with time [113]. Time domain OCT has a wider scan range but relatively lower resolution. With the development of spectral OCT, which provides an axial resolution of 3 μm [114], the limbal structure can be better elucidated in normal and pathological conditions [110, 115, 116].

5.1.2.2. Ocular surface structure

5.1.2.2.1. Corneal and limbal epithelium: AS-OCT provides two methods to measure epithelium thickness. The thickness of the epithelial cell layer within a 6-mm diameter of the central cornea can be automatically measured (Fig. 2A, 2E). The thickness of epithelium, either central cornea or limbal area, can also be manually measured on cross-sectional images (Fig. 2B, 2F) [110]. AS-OCT can measure the epithelial thickness in normal eyes [110, 117] and in eyes with various ocular surface disorders [118, 119]. In LSCD, the thickness of limbal epithelium measured by AS-OCT decreases significantly (Fig. 2D–2F) [87], which is consistent with the findings of confocal imaging [70]. The limbal epithelial thinning correlates with the damage to the palisades of Vogt in LSCD. However, the application of AS-OCT to study the alterations of corneal epithelial thickness in LSCD has not yet been fully developed [70]. The irregularity of the epithelium, the reflectivity alterations of the epithelial layer, and interference caused by hyper-reflective fibrovascular tissue underneath the epithelium in LSCD are all factors that reduce the discrimination of the epithelial layer from the underlying subepithelial scar or anterior stromal haze on the OCT images. These limitations could be resolved by a newer generation of OCT with an ultra-higher resolution.

5.1.2.2.2. The palisades of Vogt: In vivo visualization of the palisades of Vogt provides information about any structural changes of the limbus in healthy and pathological conditions. Spectral domain OCT has been reported to visualize the palisades of Vogt (Fig.

2C) [120]. This technique may enhance targeted limbal biopsies for transplantation [121]. However, as mentioned above, the palisades of Vogt may be absent in eyes with normal LSC function. IVCM is a more sensitive tool to locate normal limbal epithelium for biopsy.

5.1.2.3. OCT angiography (OCTA): Recent technological developments have increased the imaging capabilities of OCT in the evaluation of vascular flow; use of OCT for this purpose is called OCT angiography (OCTA). This method visualizes vessels via motion contrast imaging of erythrocyte movement across sequential B-scans [122]. In a preliminary study, OCTA acquired images of the cornea and limbal vasculature with substantial consistency [123]. Although the utilization of OCTA in the diagnosis of LSCD is probably limited because corneal neovascularization is not a specific sign of LSCD, it might be a promising tool to quantify the extent of corneal neovascularization.

5.1.3. Three-dimensional imaging of cornea and limbus—With recent improvement of hardware and software in quantitative corneal imaging by IVCM, three-dimensional images of the cornea and limbus can be obtained. These images allow measurement of corneal sublayer thicknesses, stromal cell and extracellular matrix backscatter, depth-dependent changes in corneal keratocyte density, and the structure of the subbasal nerve plexus [124]. The development of image acquisition, reconstruction, and analysis techniques should further expand the applications of IVCM in the diagnosis of LSCD.

With the progress of volumetric OCT and computer-assisted three-dimensional reconstruction technology, spectral domain OCT has recently been shown to have the capability of visualizing the three-dimensional structure of the limbal area by using reconstructed volumetric images that include the palisades of Vogt, blood vessels, lymphoid channels, Schlemm's canal, trabecular meshwork and corneal nerve fiber bundles [125–128]. The palisades of Vogt appear to be connected in the stromal layer as deep as 120 μm below the epithelial surface. These deep invasions of epithelium form an elaborate network [82]. This finding suggests that LSCs are likely to be located very deep in the limbal stroma.

Three-dimensional images of the limbus could provide important structural information on the LSC niche in both normal and pathologic conditions. The structural information could be used as a new parameter to detect residual LSCs and quantify the severity of LSCD.

5.2. Molecular methods

Direct histological staining (e.g., H&E staining and Papanicolaou staining) of impression cytology specimens is used to evaluate the morphology of the epithelium. However, histology cannot distinguish conjunctival epithelial cells from corneal epithelial cells without cell-specific markers.

5.2.1. Molecular biomarkers—Cytokeratins are a group of water-insoluble proteins that form intermediate filaments in epithelial cells and are expressed in distinct patterns during epithelial development and differentiation. Immunocytochemical analysis of impression cytology specimens can identify the specific type of cytokeratin present and hence determine

the type of epithelium. Cytokeratin profiles have been used as markers of epithelial origins and as a supplementary diagnostic tool in some studies of LSCD [129, 130].

Table 3 summarizes the biomarkers that have been used in the diagnosis of LSCD and methods to detect them. Cytokeratin 3 and 12 are regarded as specific markers of differentiated corneal epithelial cells, whereas cytokeratin 19 and mucin 1(MUC1) are reportedly conjunctiva-specific markers [54, 81, 131]. However, other reports have shown that cytokeratin 19 is expressed in the limbal and peripheral corneal epithelium and MUC 1 is expressed throughout the entire ocular surface in the normal human eye [132, 133]. Keratin 3 is also expressed in the conjunctiva [81]. Therefore, cytokeratin 3 is less specific than cytokeratin 12 to identify corneal epithelium, and keratin 19 and mucin 1 are not specific for conjunctival epithelium. In contrast, cytokeratin 7 and cytokeratin 13 are expressed in the conjunctival epithelium but not in the corneal epithelium [134, 135]; thus, these two proteins are more specific markers of conjunctival epithelial cells than cytokeratin 19 and MUC1. Cytokeratin 15 has also been reported as the specific marker of conjunctival epithelial cells [136]. However, its application in impression cytology is under investigation. Mucin 5AC is a specific marker of goblet cells [132] which has been used to detect goblet cells.

5.2.2. Methods to detect the molecular biomarkers—The traditional technique to detect cytokeratin is immunohistochemistry. Flow cytometric analysis of cells collected by impression cytology is a new approach [137]. Other molecular analytical methods, such as RT-PCR to detect the transcript of Mucin 5AC, are more sensitive and objective than the immunohistochemistry staining [132, 138–140].

In recent years, the protein/cytokine analysis of tears has been performed in patients with congenital aniridia using high-performance liquid chromatography, two-dimensional electrophoresis, and liquid chromatography-tandem mass spectrometry [141, 142]. Tear acquisition is easier to perform and less traumatic to the epithelium than impression cytology. The diagnostic value of these proteins/cytokines in tear still needs further investigation and validation because aniridia accounts for only a very small portion of LSCD.

The use of specific markers of conjunctival and corneal epithelia and the application of new techniques to detect these markers increases the specificity and sensitivity of traditional impression cytology. Optimization of these molecular techniques is needed to verify their utility as diagnostic tests. The diagnosis of LSCD will be more reliable using the combination of molecular diagnostic tests and in vivo imaging.

6. Future Developments

The characterization of the cellular structure of the cornea and limbus in healthy eyes using in vivo imaging has increased our understanding of pathophysiology of external eye diseases [85, 110, 143, 144]. Cellular changes in the cornea and limbus occur in LSCD and have been quantified by both IVCM and AS-OCT. Basal cell density, subbasal nerve density and epithelial thickness are three quantifiable measures that have been shown to correlate with

the severity of LSCD. With further improvement in image resolution and image analysis software, these quantifiable parameters could be further optimized to establish a threshold level that indicates the occurrence of LSCD and to classify the severity of LSCD.

The three-dimensional structure of the limbus can be mapped by IVCM and AS-OCT, and the number of any residual limbal epithelial cells located in deep limbal crypts/lacunae could be identified. In addition, these residual LSCs could be collected by targeted biopsy for autologous LSC therapy in severe LSCD.

A precise diagnostic test using molecular markers to detect conjunctival epithelial cells on the cornea will be important in confirming the diagnosis of LSCD. A combination of the molecular diagnostic tests, the grading of clinical signs, and the detection of microstructural changes could lead to a precise staging of LSCD and assessment of the clinical outcome of LSC therapy in the future.

The treatment approaches for different severity levels of LSCD are different. In partial LSCD, elimination of ongoing insults to the existing LSCs and optimization of the health of the ocular surface should be the first steps in recovering the LSC population from the remaining LSC pool and restoring LSC function. These initial steps would not require LSC transplantation. It is likely that only in severe or total LSCD, transplantation of LSCs will be necessary. The degree of LSCD that requires LSC transplantation remains to be established. The same criteria to stage LSCD would be used to assess the clinical outcome of different therapies and make future improvement of these therapies possible.

7. Summary

The current diagnostic methods and criteria for LSCD are based solely on clinical examination and traditional impression cytology. They are not accurate and do not permit the quantification of LSC function or LSCD. There is a lack of consensus in the current diagnostic approaches for LSCD. In vivo imaging devices are powerful tools to analyze and quantify the in vivo dynamic changes of the ocular surface structure at the cellular level. A set of standardized criteria can be established by using a combination of grading of clinical presentation, quantitative analysis of ocular surface structural changes, and detection of molecular biomarkers to accurately diagnose and quantify LSCD.

Acknowledgments

This study was supported by an unrestricted grant from Research to Prevent Blindness. SXD received grant support from National Eye Institute (5P30EY000331 and R01EY021797), California Institute for Regenerative Medicine (TR2-01768, CLIN1-08686).

References

1. Van Buskirk EM. The anatomy of the limbus. Eye (Lond). 1989; 3:101–8. [PubMed: 2695343]
2. Ramos T, Scott D, Ahmad S. An update on ocular surface epithelial stem cells: cornea and conjunctiva. Stem Cells Int. 2015; 2015:601731. [PubMed: 26146504]
3. Tseng SC. Concept and application of limbal stem cells. Eye (Lond). 1989; 3:141–57. [PubMed: 2695347]

4. Joe AW, Yeung SN. Concise review: identifying limbal stem cells: classical concepts and new challenges. Stem Cells Transl Med. 2014; 3:318–22. [PubMed: 24327757]
5. Sangwan VS. Limbal stem cells in health and disease. Biosci Rep. 2001; 21:385–405. [PubMed: 11900318]
6. Ordonez P, Di Girolamo N. Limbal epithelial stem cells: role of the niche microenvironment. Stem Cells. 2012; 30:100–7. [PubMed: 22131201]
7. Di Girolamo N. Moving epithelia: Tracking the fate of mammalian limbal epithelial stem cells. Prog Retin Eye Res. 2015; 48:203–25. [PubMed: 25916944]
8. Zhao J, Mo V, Nagasaki T. Distribution of label-retaining cells in the limbal epithelium of a mouse eye. J Histochem Cytochem. 2009; 57:177–85. [PubMed: 19001638]
9. Dziasko MA, Daniels JT. Anatomical features and cell-cell interactions in the human limbal epithelial stem cell niche. Ocul Surf. 2016; 14:322–30. [PubMed: 27151422]
10. Castro-Munozledo F. Review: Corneal epithelial stem cells, their niche and wound healing. Mol Vis. 2013; 19:1600–13. [PubMed: 23901244]
11. Funderburgh JL, Funderburgh ML, Du Y. Stem cells in the limbal stroma. Ocul Surf. 2016; 14:113–20. [PubMed: 26804252]
12. Yamada K, Young RD, Lewis PN, Shinomiya K, Meek KM, Kinoshita S, et al. Mesenchymal-epithelial cell interactions and proteoglycan matrix composition in the presumptive stem cell niche of the rabbit corneal limbus. Mol Vis. 2015; 21:1328–39. [PubMed: 26788025]
13. Shortt AJ, Secker GA, Munro PM, Khaw PT, Tuft SJ, Daniels JT. Characterization of the limbal epithelial stem cell niche: novel imaging techniques permit in vivo observation and targeted biopsy of limbal epithelial stem cells. Stem Cells. 2007; 25:1402–9. [PubMed: 17332511]
14. Dua HS, Shanmuganathan VA, Powell-Richards AO, Tighe PJ, Joseph A. Limbal epithelial crypts: a novel anatomical structure and a putative limbal stem cell niche. Br J Ophthalmol. 2005; 89:529–32. [PubMed: 15834076]
15. Sejpal K, Bakhtiari P, Deng SX. Presentation, diagnosis and management of limbal stem cell deficiency. Middle East Afr J Ophthalmol. 2013; 20:5–10. [PubMed: 23580847]
16. Dua HS, Saini JS, Azuara-Blanco A, Gupta P. Limbal stem cell deficiency: concept, aetiology, clinical presentation, diagnosis and management. Indian J Ophthalmol. 2000; 48:83–92. [PubMed: 11116520]
17. Dua HS, Miri A, Alomar T, Yeung AM, Said DG. The role of limbal stem cells in corneal epithelial maintenance: testing the dogma. Ophthalmology. 2009; 116:856–63. [PubMed: 19410942]
18. Le Q, Deng SX, Xu J. In vivo confocal microscopy of congenital aniridia-associated keratopathy. Eye (Lond). 2013; 27:763–6. [PubMed: 23579408]
19. Skeens HM, Brooks BP, Holland EJ. Congenital aniridia variant: minimally abnormal irides with severe limbal stem cell deficiency. Ophthalmology. 2011; 118:1260–4. [PubMed: 21376398]
20. Merchant A, Zhao TZ, Foster CS. Chronic keratoconjunctivitis associated with congenital dyskeratosis and erythrokeratodermia variablis. Ophthalmology. 1998; 105:1286–91. [PubMed: 9663235]
21. Di Iorio E, Kaye SB, Ponzin D, Barbaro V, Ferrari S, Böhm E, et al. Limbal stem cell deficiency and ocular phenotype in ectrodactyly-ectodermal dysplasia-clefting syndrome caused by p63 mutations. Ophthalmology. 2012; 119:74–83. [PubMed: 21959367]
22. Aslan D, Akata R. Dyskeratosis congenita and limbal stem cell deficiency. Exp Eye Res. 2010; 90:472–3. [PubMed: 20036237]
23. Strungaru MH, Mah D, Chan CC. Focal limbal stem cell deficiency in Turner syndrome: report of two patients and review of the literature. Cornea. 2014; 33:207–9. [PubMed: 24342891]
24. Cortes M, Lambiase A, Sacchetti M, Aronni S, Bonini S. Limbal stem cell deficiency associated with LADD syndrome. Arch Ophthalmol. 2005; 123:691–4. [PubMed: 15883293]
25. Fernandes M, Sangwan VS, Vemuganti GK. Limbal stem cell deficiency and xeroderma pigmentosum: a case report. Eye (Lond). 2004; 18:741–3. [PubMed: 15238945]
26. Ahmad S. Concise review: limbal stem cell deficiency, dysfunction, and distress. Stem Cells Transl Med. 2012; 1:110–5. [PubMed: 23197757]

27. Le QH, Wang WT, Hong JX, Sun XH, Zheng TY, Zhu WQ, et al. An in vivo confocal microscopy and impression cytology analysis of goblet cells in patients with chemical burns. Invest Ophthalmol Vis Sci. 2010; 51:1397–400. [PubMed: 20185840]
28. Bobba S, Di Girolamo N, Mills R, Daniell M, Chan E, Harkin DG, et al. Nature and incidence of severe limbal stem cell deficiency in Australia and New Zealand. Clin Exp Ophthalmol. 2017; 45:174–81. [PubMed: 27505295]
29. Eschle-Meniconi M, Ahmad S, Foster C. Mucous membrane pemphigoid: an update. Curr Opin Ophthalmol. 2005; 16:303–7. [PubMed: 16175044]
30. Catt CJ, Hamilton GM, Fish J, Mireskandari K, Ali A. Ocular manifestations of Stevens-Johnson syndrome and toxic epidermal necrolysis in children. Am J Ophthalmol. 2016; 166:68–75. [PubMed: 27018234]
31. Vera LS, Gueudry J, Delcampe A, Roujeau JC, Brasseur G, Muraine M. In vivo confocal microscopic evaluation of corneal changes in chronic Stevens-Johnson syndrome and toxic epidermal necrolysis. Cornea. 2009; 28:401–7. [PubMed: 19411958]
32. Sivaraman KR, Jivrajka RV, Soin K, Bouchard CS, Movahedan A, Shorter E, et al. Superior limbic keratoconjunctivitis-like inflammation in patients with chronic graft-versus-host disease. Ocul Surf. 2016; 14:393–400. [PubMed: 27179980]
33. Le Q, Wang Y, Xu J. In vivo confocal microscopy of long-standing mixed-form vernal keratoconjunctivitis. Ocul Immunol Inflamm. 2010; 18:349–51. [PubMed: 20818997]
34. Sangwan VS, Jain V, Vemuganti GK, Murthy SI. Vernal keratoconjunctivitis with limbal stem cell deficiency. Cornea. 2011; 30:491–6. [PubMed: 21598432]
35. Capella MJ, Alvarez de Toledo J, de la Paz MF. Limbal stem cell deficiency following multiple intravitreal injections. Arch Soc Esp Oftalmol. 2011; 86:89–92. [PubMed: 21511104]
36. Ding X, Bishop RJ, Herzlich AA, Patel M, Chan CC. Limbal stem cell deficiency arising from systemic chemotherapy with hydroxycarbamide. Cornea. 2009; 28:221–3. [PubMed: 19158571]
37. Kim K, Kim W. Limbal stem cell deficiency associated with the anticancer drug S-1. Optom Vis Sci. 2015; 92:S10–3. [PubMed: 25756340]
38. Nghiem-Buffet MH, Gatinel D, Jacquot F, Chaine G, Hoang-Xuan T. Limbal stem cell deficiency following phototherapeutic keratectomy. Cornea. 2003; 22:482–4. [PubMed: 12827057]
39. Lichtinger A, Pe'er J, Frucht-Pery J, Solomon A. Limbal stem cell deficiency after topical mitomycin C therapy for primary acquired melanosis with atypia. Ophthalmology. 2010; 117:431–7. [PubMed: 20060167]
40. Sauder G, Jonas JB. Limbal stem cell deficiency after subconjunctival mitomycin C injection for trabeculectomy. Am J Ophthalmol. 2006; 141:1129–30. [PubMed: 16765685]
41. Baradaran-Rafii A, Javadi MA, Rezaei Kanavi M, Eslani M, Jamali H, Karimian F. Limbal stem cell deficiency in chronic and delayed-onset mustard gas keratopathy. Ophthalmology. 2010; 117:246–52. [PubMed: 20018379]
42. Chan CC, Holland EJ. Severe limbal stem cell deficiency from contact lens wear: patient clinical features. Am J Ophthalmol. 2013; 155:544–9. [PubMed: 23218703]
43. Rossen J, Amram A, Milani B, Park D, Harthan J, Joslin C, et al. Contact lens-induced limbal stem cell deficiency. Ocul Surf. 2016; 14:419–34. [PubMed: 27480488]
44. Bonini S, Rama P, Olzi D, Lambiase A. Neurotrophic keratitis. Eye (Lond). 2003; 17:989–95. [PubMed: 14631406]
45. dos Paris FS, Gonçalves ED, de Barros JN, Campos MS, Sato EH, Gomes JA. Impression cytology findings in bullous keratopathy. Br J Ophthalmol. 2010; 94:773–6. [PubMed: 19965819]
46. Gupta N, Sachdev R, Tandon R. Ocular surface squamous neoplasia in xeroderma pigmentosum: clinical spectrum and outcome. Graefes Arch Clin Exp Ophthalmol. 2011; 249:1217–21. [PubMed: 21484462]
47. Masse K, Bhamra S, Eason R, Dale N, Jones EA. Purine-mediated signaling triggers eye development. Nature. 2007; 449:1058–62. [PubMed: 17960245]
48. Li G, Xu F, Zhu J, Krawczyk M, Zhang Y, Yuan J, et al. Transcription factor PAX6 (Paired Box 6) controls limbal stem cell lineage in development and disease. J Biol Chem. 2015; 290:20448–54. [PubMed: 26045558]

49. Douvaras P, Mort RL, Edwards D, Ramaesh K, Dhillon B, Morley SD, et al. Increased corneal epithelial turnover contributes to abnormal homeostasis in the Pax6(+/−) mouse model of aniridia. PLoS One. 2013; 8:e71117. [PubMed: 23967157]
50. Lin Z, He H, Zhou T, Liu X, Wang Y, He H, et al. A mouse model of limbal stem cell deficiency induced by topical medication with the preservative benzalkonium chloride. Invest Ophthalmol Vis Sci. 2013; 54:6314–25. [PubMed: 23963168]
51. Kadar T, Turetz J, Fishbine E, Sahar R, Chapman S, Amir A. Characterization of acute and delayed ocular lesions induced by sulfur mustard in rabbits. Curr Eye Res. 2001; 22:42–53. [PubMed: 11402378]
52. Ruff AL, Jarecke AJ, Hilber DJ, Rothwell CC, Beach SL, Dillman JF 3rd. Development of a mouse model for sulfur mustard-induced ocular injury and long-term clinical analysis of injury progression. Cutan Ocul Toxicol. 2013; 32:140–9. [PubMed: 23106216]
53. Deng SX, Sejpal KD, Tang Q, Aldave AJ, Lee OL, Yu F. Characterization of limbal stem cell deficiency by in vivo laser scanning confocal microscopy: a microstructural approach. Arch Ophthalmol. 2012; 130:440–5. [PubMed: 22159172]
54. Sacchetti M, Lambiase A, Cortes M, Sgrulletta R, Bonini S, Merlo D, et al. Clinical and cytological findings in limbal stem cell deficiency. Graefes Arch Clin Exp Ophthalmol. 2005; 243:870–6. [PubMed: 15778841]
55. Dua HS, Joseph A, Shanmuganathan VA, Jones RE. Stem cell differentiation and the effects of deficiency. Eye (Lond). 2003; 17:877–85. [PubMed: 14631392]
56. Dua HS. The conjunctiva in corneal epithelial wound healing. Br J Ophthalmol. 1998; 82:1407–11. [PubMed: 9930272]
57. Zheng T, Xu J. Age-related changes of human limbus on in vivo confocal microscopy. Cornea. 2008; 27:782–6. [PubMed: 18650663]
58. Lim P, Fuchsluger TA, Jurkunas UV. Limbal stem cell deficiency and corneal neovascularization. Semin Ophthalmol. 2009; 24:139–48. [PubMed: 19437349]
59. Shortt AJ, Bunce C, Levis HJ, Blows P, Doré CJ, Vernon A, et al. Three-year outcomes of cultured limbal epithelial allografts in aniridia and Stevens-Johnson syndrome evaluated using the Clinical Outcome Assessment in Surgical Trials assessment tool. Stem Cells Transl Med. 2014; 3:265–75. [PubMed: 24443006]
60. Sandali O, Gaujoux T, Goldschmidt P, Ghoubay-Benallaoua D, Laroche L, Borderie VM. Infectious keratitis in severe limbal stem cell deficiency: characteristics and risk factors. Ocul Immunol Inflamm. 2012; 20:182–9. [PubMed: 22537286]
61. Kang BS, Kim MK, Wee WR, Oh JY. Infectious keratitis in limbal stem cell deficiency: Stevens-Johnson syndrome versus chemical burn. Cornea. 2016; 35:51–5. [PubMed: 26555593]
62. Calonge M, Diebold Y, Sáez V, Enríquez de Salamanca A, García-Vázquez C, Corrales RM, et al. Impression cytology of the ocular surface: a review. Exp Eye Res. 2004; 78:457–72. [PubMed: 15106925]
63. Singh R, Joseph A, Umapathy T, Tint NL, Dua HS. Impression cytology of the ocular surface. Br J Ophthalmol. 2005; 89:1655–9. [PubMed: 16299150]
64. Araújo AL, Ricardo JR, Sakai VN, Barros JN, Gomes JÁ. Impression cytology and in vivo confocal microscopy in corneas with total limbal stem cell deficiency. Arq Bras Oftalmol. 2013; 76:305–8. [PubMed: 24232946]
65. Puangsricharern V, Tseng SC. Cytologlogic evidence of corneal diseases with limbal stem cell deficiency. Ophthalmology. 1995; 102:1476–85. [PubMed: 9097795]
66. Kenyon KR, Tseng SC. Limbal autograft transplantation for ocular surface disorders. Ophthalmology. 1989; 96:709–22. [PubMed: 2748125]
67. Doughty MJ. Goblet cells of the normal human bulbar conjunctiva and their assessment by impression cytology sampling. Ocul Surf. 2012; 10:149–69. [PubMed: 22814643]
68. Jawaheer L, Anijeet D, Ramaesh K. Diagnostic criteria for limbal stem cell deficiency-A systematic literature review. Surv Ophthalmol. 2017; 62:522–32. [PubMed: 27856177]
69. Chan EH, Chen L, Rao JY, Yu F, Deng SX. Limbal basal cell density decreases in limbal stem cell deficiency. Am J Ophthalmol. 2015; 160:678–84. [PubMed: 26149968]

70. Chan EH, Chen L, Yu F, Deng SX. Epithelial thinning in limbal stem cell deficiency. Am J Ophthalmol. 2015; 160:669–77. [PubMed: 26163009]
71. Chan E, Le Q, Codriansky A, Hong J, Xu J, Deng SX. Existence of normal limbal epithelium in eyes with clinical signs of total limbal stem cell deficiency. Cornea. 2016; 35:1483–7. [PubMed: 27362882]
72. Goldberg MF. In vivo confocal microscopy and diagnosis of limbal stem cell deficiency. Photographing the palisades of Vogt and limbal stem cells. Am J Ophthalmol. 2013; 156:205–6. [PubMed: 23791376]
73. Fatima A, Iftekhar G, Sangwan VS, Vemuganti GK. Ocular surface changes in limbal stem cell deficiency caused by chemical injury: a histologic study of excised pannus from recipients of cultured corneal epithelium. Eye (Lond). 2008; 22:1161–7. [PubMed: 17558385]
74. López-García JS, Rivas Jara L, García-Lozano CI, Conesa E, de Juan IE, Murube del Castillo J. Ocular features and histopathologic changes during follow-up of toxic epidermal necrolysis. Ophthalmology. 2011; 118:265–71. [PubMed: 20884054]
75. Nelson JD, Wright JC. Conjunctival goblet cell densities in ocular surface disease. Arch Ophthalmol. 1984; 102:1049–51. [PubMed: 6378156]
76. Altinors DD, Bozbeyoglu S, Karabay G, Akova YA. Evaluation of ocular surface changes in a rabbit dry eye model using a modified impression cytology technique. Curr Eye Res. 2007; 32:301–7. [PubMed: 17453951]
77. Hong J, Zhu W, Zhuang H, Xu J, Sun X, Le Q, et al. In vivo confocal microscopy of conjunctival goblet cells in patients with Sjogren's Syndrome dry eye. Br J Ophthalmol. 2010; 94:1454–8. [PubMed: 19955202]
78. Chen P, Zhou Q, Wang J, Zhao X, Duan H, Wang Y, et al. Characterization of the corneal surface in limbal stem cell deficiency and after transplantation of cultured allogeneic limbal epithelial cells. Graefes Arch Clin Exp Ophthalmol. 2016; 254:1765–77. [PubMed: 27313163]
79. Daya SM, Watson A, Sharpe JR, Giledi O, Rowe A, Martin R, et al. Outcomes and DNA analysis of ex vivo expanded stem cell allograft for ocular surface reconstruction. Ophthalmology. 2005; 112:470–7. [PubMed: 15745776]
80. Kobayashi A, Sugiyama K. In vivo corneal confocal microscopic findings of palisades of Vogt and its underlying limbal stroma. Cornea. 2005; 24:435–7. [PubMed: 15829801]
81. Barbaro V, Ferrari S, Fasolo A, Pedrotti E, Marchini G, Sbabo A, et al. Evaluation of ocular surface disorders: a new diagnostic tool based on impression cytology and confocal laser scanning microscopy. Br J Ophthalmol. 2010; 94:926–32. [PubMed: 19740872]
82. Miri A, Al-Aqaba M, Otri AM, Fares U, Said DG, Faraj LA, et al. In vivo confocal microscopic features of normal limbus. Br J Ophthalmol. 2012; 96:530–6. [PubMed: 22328815]
83. Cruzat A, Pavan-Langston D, Hamrah P. In vivo confocal microscopy of corneal nerves: analysis and clinical correlation. Semin Ophthalmol. 2010; 25:171–7. [PubMed: 21090996]
84. Falke K, Prakasam RK, Guthoff RF, Stachs O. In vivo imaging of limbal epithelium and palisades of Vogt. Klin Monbl Augenheilkd. 2012; 229:1185–90. [PubMed: 23258669]
85. Niederer RL, McGhee CN. Clinical in vivo confocal microscopy of the human cornea in health and disease. Prog Retin Eye Res. 2010; 29:30–58. [PubMed: 19944182]
86. Lagali N, Edén U, Utheim TP, Chen X, Riise R, Dellby A, et al. In vivo morphology of the limbal palisades of vogt correlates with progressive stem cell deficiency in aniridia-related keratopathy. Invest Ophthalmol Vis Sci. 2013; 54:5333–42. [PubMed: 23860752]
87. Le Q, Yang Y, Deng SX, Xu J. Correlation between the existence of the palisades of Vogt and limbal epithelial thickness in limbal stem cell deficiency. Clin Exp Ophthalmol. 2017; 45:224–31. [PubMed: 27591548]
88. Miri A, Alomar T, Nubile M, Al-Aqaba M, Lanzini M, Fares U, et al. In vivo confocal microscopic findings in patients with limbal stem cell deficiency. Br J Ophthalmol. 2012; 96:523–9. [PubMed: 22328810]
89. Nubile M, Lanzini M, Miri A, Pocobelli A, Calienno R, Curcio C, et al. In vivo confocal microscopy in diagnosis of limbal stem cell deficiency. Am J Ophthalmol. 2013; 155:220–32. [PubMed: 23127748]

90. Zhu W, Hong J, Zheng T, Le Q, Xu J, Sun X. Age-related changes of human conjunctiva on in vivo confocal microscopy. Br J Ophthalmol. 2010; 94:1448–53. [PubMed: 20494916]

91. Efron N, Al-Dossari M, Pritchard N. In vivo confocal microscopy of the bulbar conjunctiva. Clin Exp Ophthalmol. 2009; 37:335–44. [PubMed: 19594558]

92. Mastropasqua L, Calienno R, Lanzini M, Nubile M, Colabelli-Gisoldi RA, De Carlo L, et al. In vivo confocal microscopy of the sclerocorneal limbus after limbal stem cell transplantation: Looking for limbal architecture modifications and cytological phenotype correlations. Mol Vis. 2016; 22:748–60. [PubMed: 27440993]

93. Cruzat A, Qazi Y, Hamrah P. In vivo confocal microscopy of corneal nerves in health and disease. Ocul Surf. 2017; 15:15–47. [PubMed: 27771327]

94. Moriez R, Abdo H, Chaumette T, Faure M, Lardeux B, Neunlist M. Neuroplasticity and neuroprotection in enteric neurons: role of epithelial cells. Biochem Biophys Res Commun. 2009; 382:577–82. [PubMed: 19302981]

95. Chuephanich P, Supiyaphun C, Aravena C, Bozkurt TK, Yu F, Deng SX. Characterization of the corneal subbasal nerve plexus in limbal stem cell deficiency. Cornea. 2017; 36:347–52. [PubMed: 27941384]

96. Long Q, Zuo YG, Yang X, Gao TT, Liu J, Li Y. Clinical features and in vivo confocal microscopy assessment in 12 patients with ocular cicatricial pemphigoid. Int J Ophthalmol. 2016; 9:730–7. [PubMed: 27275431]

97. Zhivov A, Winter K, Hovakimyan M, Peschel S, Harder V, Schober HC, et al. Imaging and quantification of subbasal nerve plexus in healthy volunteers and diabetic patients with or without retinopathy. PLoS One. 2013; 8:e52157. [PubMed: 23341892]

98. Bitirgen G, Akpinar Z, Malik RA, Ozkagnici A. Use of corneal confocal microscopy to detect corneal nerve loss and increased dendritic cells in patients with multiple sclerosis. JAMA Ophthalmol. 2017; 135:777–82. [PubMed: 28570722]

99. Gatzioufas Z, Labiris G, Hafezi F, Schnaidt A, Pajic B, Langenbucher A, et al. Corneal sensitivity and morphology of the corneal subbasal nerve plexus in primary congenital glaucoma. Eye (Lond). 2014; 28:466–71. [PubMed: 24480838]

100. Pahuja NK, Shetty R, Nuijts RM, Agrawal A, Ghosh A, Jayadev C, et al. An in vivo confocal microscopic study of corneal nerve morphology in unilateral keratoconus. Biomed Res Int. 2016; 2016:5067853. [PubMed: 26904679]

101. Bucher F, Adler W, Lehmann HC, Hos D, Steven P, Cursiefen C, et al. Corneal nerve alterations in different stages of Fuchs' endothelial corneal dystrophy: an in vivo confocal microscopy study. Graefes Arch Clin Exp Ophthalmol. 2014; 252:1119–26. [PubMed: 24874747]

102. Bucher F, Hos D, Matthaei M, Steven P, Cursiefen C, Heindl LM. Corneal nerve alterations after Descemet membrane endothelial keratoplasty: an in vivo confocal microscopy study. Cornea. 2014; 33:1134–9. [PubMed: 25222002]

103. Zhivov A, Winter K, Peschel S, Stachs O, Wree A, Hildebrandt G, et al. Changes in the micromorphology of the corneal subbasal nerve plexus in patients after plaque brachytherapy. Radiat Oncol. 2013; 8:136. [PubMed: 23759072]

104. Bouheraoua N, Hrarat L, Parsa CF, Akesbi J, Sandali O, Goemaere I, et al. Decreased corneal sensation and subbasal nerve density, and thinned corneal epithelium as a result of 360-degree laser retinopexy. Ophthalmology. 2015; 122:2095–102. [PubMed: 26189186]

105. Nombela-Palomo M, Felipe-Marquez G, Hernandez-Verdejo JL, Nieto-Bona A. Short-term effects of overnight orthokeratology on corneal sub-basal nerve plexus morphology and corneal sensitivity. Eye Contact Lens. 2016 May 26. Epub ahead of print.

106. Xiang J, Le Q, Li Y, Xu J. In vivo confocal microscopy of early corneal epithelial recovery in patients with chemical injury. Eye (Lond). 2015; 29:1570–8. [PubMed: 26381093]

107. Chidambaranathan GP, Mathews S, Panigrahi AK, Mascarenhas J, Prajna NV, Muthukkaruppan V. In vivo confocal microscopic analysis of limbal stroma in patients with limbal stem cell deficiency. Cornea. 2015; 34:1478–86. [PubMed: 26312622]

108. Dziasko MA, Armer HE, Levis HJ, Shortt AJ, Tuft S, Daniels JT. Localisation of epithelial cells capable of holoclone formation in vitro and direct interaction with stromal cells in the native human limbal crypt. PLoS One. 2014; 9:e94283. [PubMed: 24714106]

109. Zarei-Ghanavati S, Ramirez-Miranda A, Deng SX. Limbal lacuna: a novel limbal structure detected by in vivo laser scanning confocal microscopy. Ophthalmic Surg Lasers Imaging. 2011; 42:e129–31. [PubMed: 22150603]
110. Yang Y, Hong J, Deng SX, Xu J. Age-related changes in human corneal epithelial thickness measured with anterior segment optical coherence tomography. Invest Ophthalmol Vis Sci. 2014; 55:5032–8. [PubMed: 25052994]
111. Izatt JA, Hee MR, Swanson EA, Lin CP, Huang D, Schuman JS, et al. Micrometer-scale resolution imaging of the anterior eye in vivo with optical coherence tomography. Arch Ophthalmol. 1994; 112:1584–9. [PubMed: 7993214]
112. Ramos JL, Li Y, Huang D. Clinical and research applications of anterior segment optical coherence tomography - a review. Clin Exp Ophthalmol. 2009; 37:81–9. [PubMed: 19016809]
113. Jancevski M, Foster CS. Anterior segment optical coherence tomography. Semin Ophthalmol. 2010; 25:317–23. [PubMed: 21091018]
114. Thomas BJ, Galor A, Nanji AA, El Sayyad F, Wang J, Dubovy SR, et al. Ultra high-resolution anterior segment optical coherence tomography in the diagnosis and management of ocular surface squamous neoplasia. Ocul Surf. 2014; 12:46–58. [PubMed: 24439046]
115. Feng Y, Simpson T. Corneal, limbal, and conjunctival epithelial thickness from optical coherence tomography. Optom Vis Sci. 2008; 85:e880–3. [PubMed: 18772715]
116. Feng Y, Simpson T. Comparison of human central cornea and limbus in vivo using optical coherence tomography. Optom Vis Sci. 2005; 82:416–9. [PubMed: 15894917]
117. Francoz M, Karamoko I, Baudouin C, Labbé A. Ocular surface epithelial thickness evaluation with spectral-domain optical coherence tomography. Invest Ophthalmol Vis Sci. 2011; 52:9116–23. [PubMed: 22025572]
118. Calabuig-Goena M, López-Miguel A, Marqués-Fernández V, Coco-Martín MB, Iglesias-Cortiñas D, Maldonado MJ. Early changes in corneal epithelial thickness after cataract surgery--pilot study. Curr Eye Res. 2016; 41:311–7. [PubMed: 25803625]
119. Cui X, Hong J, Wang F, Deng SX, Yang Y, Zhu X, et al. Assessment of corneal epithelial thickness in dry eye patients. Optom Vis Sci. 2014; 91:1446–54. [PubMed: 25279779]
120. Haagdorens M, Behaegel J, Rozema J, Van Gerwen V, Michiels S, Ní Dhubhghaill S, et al. A method for quantifying limbal stem cell niches using OCT imaging. Br J Ophthalmol. 2017; 101:1250–5. [PubMed: 28228408]
121. Espandar L, Steele JF, Lathrop KL. Optical coherence tomography imaging of the palisades of Vogt to assist clinical evaluation and surgical planning in a case of limbal stem-cell deficiency. Eye Contact Lens. 2017; 43:e19–21. [PubMed: 26783982]
122. Spaide RF, Klancnik JM Jr, Cooney MJ. Retinal vascular layers imaged by fluorescein angiography and optical coherence tomography angiography. JAMA Ophthalmol. 2015; 133:45–50. [PubMed: 25317632]
123. Ang M, Sim DA, Keane PA, Sng CC, Egan CA, Tufail A, et al. optical coherence tomography angiography for anterior segment vasculature imaging. Ophthalmology. 2015; 122:1740–7. [PubMed: 26088621]
124. Petroll WM, Robertson DM. In vivo confocal microscopy of the cornea: new developments in image acquisition, reconstruction, and analysis using the HRT-Rostock corneal module. Ocul Surf. 2015; 13:187–203. [PubMed: 25998608]
125. Bizheva K, Hutchings N, Sorbara L, Moayed AA, Simpson T. In vivo volumetric imaging of the human corneo-scleral limbus with spectral domain OCT. Biomed Opt Express. 2011; 2:1794–1802. [PubMed: 21750758]
126. Lathrop KL, Gupta D, Kagemann L, Schuman JS, Sundarraj N. Optical coherence tomography as a rapid, accurate, noncontact method of visualizing the palisades of Vogt. Invest Ophthalmol Vis Sci. 2012; 53:1381–7. [PubMed: 22266521]
127. Li P, An L, Reif R, Shen TT, Johnstone M, Wang RK. In vivo microsctructural and microvascular imaging of human corneo-scleral limbus using optical coherence tomography. Biomed Opt Express. 2011; 2:3109–18. [PubMed: 22076271]

128. Grieve K, Ghoubay D, Georgeon C, Thouvenin O, Bouheraoua N, Paques M, et al. Three-dimensional structure of the mammalian limbal stem cell niche. Exp Eye Res. 2015; 140:75–84. [PubMed: 26297801]

129. Ricardo JR, Cristovam PC, Filho PA, Farias CC, de Araujo AL, Loureiro RR, et al. Transplantation of conjunctival epithelial cells cultivated ex vivo in patients with total limbal stem cell deficiency. Cornea. 2013; 32:221–8. [PubMed: 22580434]

130. Kawashima M, Kawakita T, Satake Y, Higa K, Shimazaki J. Phenotypic study after cultivated limbal epithelial transplantation for limbal stem cell deficiency. Arch Ophthalmol. 2007; 125:1337–44. [PubMed: 17923540]

131. Donisi PM, Rama P, Fasolo A, Ponzin D. Analysis of limbal stem cell deficiency by corneal impression cytology. Cornea. 2003; 22:533–8. [PubMed: 12883346]

132. Poli M, Burillon C, Auxenfans C, Rovere MR, Damour O. Immunocytochemical diagnosis of limbal stem cell deficiency: Comparative study analysis of current corneal and conjunctival biomarkers. Cornea. 2015; 34:817–23. [PubMed: 25970431]

133. Gipson IK, Spurr-Michaud S, Argüeso P, Tisdale A, Ng TF, Russo CL. Mucin gene expression in immortalized human corneal-limbal and conjunctival epithelial cell lines. Invest Ophthalmol Vis Sci. 2003; 44:2496–506. [PubMed: 12766048]

134. Ramirez-Miranda A, Nakatsu MN, Zarei-Ghanavati S, Nguyen CV, Deng SX. Keratin 13 is a more specific marker of conjunctival epithelium than keratin 19. Mol Vis. 2011; 17:1652–61. [PubMed: 21738394]

135. Poli M, Janin H, Justin V, Auxenfans C, Burillon C, Damour O. Keratin 13 immunostaining in corneal impression cytology for the diagnosis of limbal stem cell deficiency. Invest Ophthalmol Vis Sci. 2011; 52:9411–5. [PubMed: 22064992]

136. Yoshida S, Shimmura S, Kawakita T, Miyashita H, Den S, Shimazaki J, et al. Cytokeratin 15 can be used to identify the limbal phenotype in normal and diseased ocular surfaces. Invest Ophthalmol Vis Sci. 2006; 47:4780–6. [PubMed: 17065488]

137. Brignole-Baudouin F, Ott AC, Warnet JM, Baudouin C. Flow cytometry in conjunctival impression cytology: a new tool for exploring ocular surface pathologies. Exp Eye Res. 2004; 78:473–81. [PubMed: 15106926]

138. Garcia I, Etxebarria J, Boto-de-Los-Bueis A, Díaz-Valle D, Rivas L, Martínez-Soroa I, et al. Comparative study of limbal stem cell deficiency diagnosis methods: detection of MUC5AC mRNA and goblet cells in corneal epithelium. Ophthalmology. 2012; 119:923–9. [PubMed: 22297031]

139. Colabelli Gisoldi RA, Pocobelli A, Villani CM, Amato D, Pellegrini G. Evaluation of molecular markers in corneal regeneration by means of autologous cultures of limbal cells and keratoplasty. Cornea. 2010; 29:715–22. [PubMed: 20489583]

140. Wang Y, Dogru M, Matsumoto Y, Ward SK, Ayako I, Hu Y, et al. The impact of nasal conjunctivochalasis on tear functions and ocular surface findings. Am J Ophthalmol. 2007; 144:930–7. [PubMed: 17916317]

141. Peral A, Carracedo G, Pintor J. Diadenosine polyphosphates in the tears of aniridia patients. Acta Ophthalmol. 2015; 93:e337–42. [PubMed: 25545014]

142. Ihnatko R, Edén U, Lagali N, Dellby A, Fagerholm P. Analysis of protein composition and protein expression in the tear fluid of patients with congenital aniridia. J Proteomics. 2013; 94:78–88. [PubMed: 24061003]

143. Parissi M, Karanis G, Randjelovic S, Germundsson J, Poletti E, Ruggeri A, et al. Standardized baseline human corneal subbasal nerve density for clinical investigation with laser-scanning in vivo confocal microscopy. Invest Ophthalmol Vis Sci. 2013; 54:7091–102. [PubMed: 24084094]

144. Niederer RL, Perumal D, Sherwin T, McGhee CN. Age-related differences in the normal human cornea: a laser scanning in vivo confocal microscopy study. Br J Ophthalmol. 2007; 91:1165–9. [PubMed: 17389741]

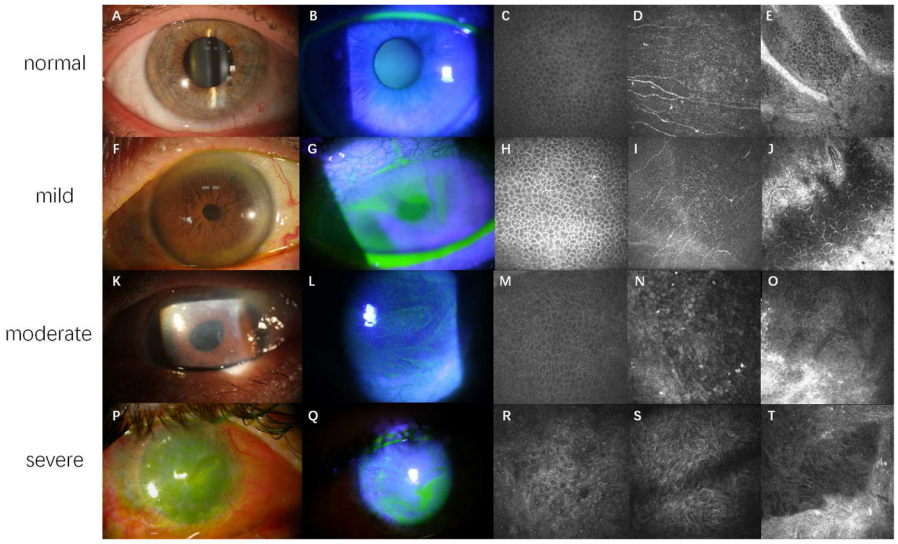

Figure 1.

Clinical presentations and confocal images of LSCD at different stages.

Figure 1A, 1F, 1K and 1P are slit lamp photos under white light. Figure 1B, 1G, 1L and 1Q are slit lamp photos under cobalt blue light. Figure 1C, 1H, 1M and 1R are confocal images of wing cells at central cornea. Figure 1D, 1I, 1N and 1S are confocal images of epithelial basal cells at central cornea. Figure 1E, 1J, 1O and 1T are confocal images of limbal epithelium and the palisades of Vogt.

Healthy corneal epithelium is transparent (A) without fluorescein staining (B). Normal wing cells (C) have a dark cytoplasm, well-defined bright borders, and no visible nuclei. Basal epithelial cells (D), which are characterized with dark cytoplasm, fairly defined cell borders and no visible nuclei, are clearly seen in normal eyes. The subbasal nerve plexus is also visible in this layer. In healthy eyes, the palisades of Vogt may be detected at the limbal area and appear as hyper-reflective, double-contour, linear structures (E). Late fluorescein staining can be detected at mild stage of LSCD, with a clear line of demarcation may be visible between the corneal and conjunctival epithelial cells in sectoral LSCD (F and G). Corneal epithelial cells in mild LSCD have less distinct borders and prominent nuclei (H and I). The density of subbasal nerve plexus decrease dramatically, along with the infiltration of dendritic cells (I). The structure of palisades of Vogt is altered even in mild LSCD. A large number of inflammatory and dendritic cells are sometimes present with blood vessels (J). Epithelial opacity (K) and persistent late fluorescein staining in a vortex pattern (L) are the signs of a more advanced stage. The morphological abnormalities of wing cells (M) and basal cells (N) at central cornea continue to progress. The degradation of subbusal nerve plexus deteriorates further (N). The palisades of Vogt are absent at limbal area, along with enlargement of limbal epithelial cells (O). Epithelial and stromal opacity, neovascularization (P), and persistent epithelial defect (Q) on the corneal surface may be present in severe or total LSCD. Metaplastic epithelial cells are visible in eyes with severe LSCD (R and S). The structures of limbus and palisades of Vogt are totally damaged (T).

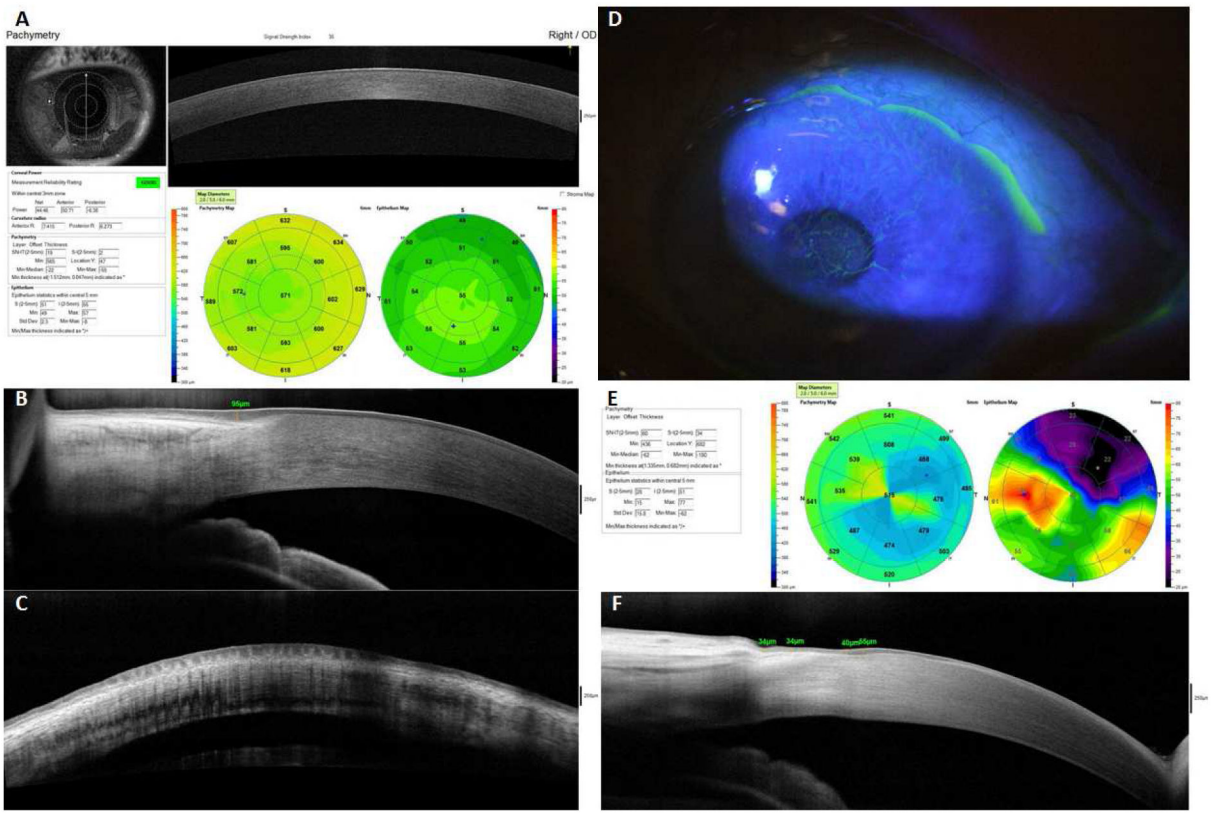

Figure 2.

AS-OCT images of normal subjects and patients with LSCD

Fig 2A–2C are taken from normal eyes. The thickness of epithelial cell layer within a 6-mm diameter of the central cornea can be automatically measured under pachymetry scan mode (A). The thickness of limbal epithelium can be manually measured on cross-sectional image (B). The palisades of Vogt are visible at limbus in normal eyes (C). Fig 2D–2F are taken from eyes with sectoral LSCD. The area with reduced epithelial thickness found in AS-OCT (E) is corresponding to the affected area shown by slit-lamp examination (D). The cross sectional images of limbus show that the thickness of limbal epithelium decreased at the affected area (F).

Table 1

Grading of LSCD based on the findings of slit lamp biomicroscopy

Report	Method	Normal (Grade 0)	Mild (Grade 1)	Moderate (Grade 2)	Severe/total (Grade 3)
Deng [53]	WL	Smooth epithelial surface	Dull corneal reflex; Superficial punctate keratitis.	Thinning of epithelial surface.	Persistent epithelial defect (or history of corneal epithelial defect), with or without vascularization of cornea.
	FLS	No staining	Stippling or late FLS.	Persistent, late FLS in a vortex pattern.	Same vortex pattern of FLS and pooling at area with epithelial abnormality.
Sacchetti[54]	WL	No epithelial alterations; No superficial neovascularization; No stromal scarring.	Epithelial haze in less than half of the sector; Superficial neovascularization involved in less than half of the sectorå Stromal scarring involved in less than half of the sector.	Epithelial haze and/or epithelial defect in more than half of the sectorå Superficial neovascularization involved in more than half of the sectorå Stromal scarring involved in more than half of the sector.	Epithelial opacity in the entire sectorå Superficial neovascularization involved in the entire Stromal sectorå scarring involved in the entire sector.
Dua[55]	WL		Loss of limbal anatomy; Irregular, thin epithelium without notable vascularization.	Irregular, thin epithelium; Filaments and erosions; Fibrovascular pannus.	Superficial and deep vascularization; Persistent epithelial defects; Fibrovascular pannus; Scarring, keratinization, and calcification.
	FLS		Stippled FLS of area covered by abnormal epithelium.	Whorls or wedges pattern FLS with the broad base toward the limbus and the narrow curving apex toward corneal center.	
*Chan[42]	WL			Epithelial opacity arising from limbus; Corneal pannus.	Corneal neovascularization; Recurrent/ persistent epithelial defects; Stromal scarring.
*Djalialian[43]	FLS		Punctate FLS following curve-like path.	Linear pattern or a confluent sheet FLS spreading centrally from limbus.	At least 6 clock hours of whorl-like FLS.
Short[59]	WL	Cornea clear; Iris detail visible; Pupil is clearly seen.	Mild haze of epithelium; Slight loss of iris; Pupil can be seen but is blurred.	Moderate haze of epithelium; No iris details visible; Pupil can just be seen with difficulty.	Severe haze of epithelium; No iris details visible; Pupil cannot be seen.

*Study focuses only on LSCD caused by contact lenses.

WL = White light. FLS = Fluorescein staining.

Table 2

Commercially available AS-OCT instrumentations at present

commercially available AS-OCT	manufacturer	platform	wave length	A scans per second	resolution	scan width
Visante OCT	Carl Zeiss Meditec, Germany	time-domain	1310nm	2000	15–20μm	16mm
slit-lamp OCT	Heidelberg Engineering GmbH, Germany	time-domain	1310nm	4000	10–15μm	15mm max
Casia SS-1000	Tomey, Japan	swept-source	1310nm	30000	10μm	16mm
RTVue	Optovue, USA	Fourier-domain	840nm	26000	5μm	2–8mm regular: 6–9mm
Cirrus OCT	Carl Zeiss Meditec, Germany	Fourier-domain	840nm	27000	5μm	max: 15.5mm
Spectralis	Heidelberg Engineering GmbH, Germany	Fourier-domain Fourier-domain	870nm	40000	3.9μm	6mm
Copernicus HR	Optopol Technology, Poland	high resolution	840nm	52000	3μm	5mm

Table 3

Biomarkers previously or currently used in the diagnosis of LSCD

biomarker	location	specificity	detection
CK3 [54, 131]	cornea	+	immunohistochemical staining
CK12 [81, 132]	cornea	+++	immunohistochemical staining
CK19 [54, 131]	conjunctiva	+	immunohistochemical staining
CK15 [136]	conjunctiva	++	immunohistochemical staining
CK7 [132]	conjunctiva	+++	immunohistochemical staining
CK13 [132, 134, 135]	conjunctiva	+++	immunohistochemical staining
MUC5AC [132, 140]	goblet cells	+++	immunohistochemical staining counterstained with hematoxylin RT-PCR
MUC1 [81]	conjunctiva (membrane-associated mucins)	+	immunohistochemical staining and immunoelectron microscopy